Kinematics of Relativistic Magnetic Reconnection

Eric G. Blackman and George B. Field
Harvard University, Cambridge, Massachusetts 02138
and Harvard-Smithsonian Center for Astrophysics, 60 Garden Street, Cambridge, Massachusetts 02138
(Received 4 August 1993)

We study the relativistic generalizations of two-dimensional Sweet-Parker and Petschek reconnection models in the context of a relativistic pair plasma. The solutions show that if the outflow velocity from the resistive region approaches the relativistic Alfvén speed, the outflow density increase from Lorentz contraction allows a much faster inflow and thus a faster rate of magnetic energy dissipation than in the nonrelativistic regime. We briefly suggest applications of this result.

PACS numbers: 52.60.+h, 52.30.−q, 95.30.Qd

The process of magnetic field reconnection and dissipation can initiate from local field configurations subject to pressure instabilities, or from external forces pushing oppositely magnetized plasmas together [1]. We recognize that the conditions under which various models of reconnection occur are not agreed upon [1–3], but that including relativity does not add any more uncertain physics *per se*. Here we study the kinematics of steady state relativistic reconnection for the two schemes depicted in Fig. 1. In each case, flows of plasma with oppositely directed magnetic fields meet along the x axis, and outflow perpendicular to the inflow ensues. We describe the difference between the schemes below.

Avoiding a singular buildup of inflow field flux on the x axis requires a topology change, which in turn requires a finite resistivity. Nonrelativistic singularity free solutions for the inflow velocity have been obtained where resistive effects are important only in a thin dissipation region (DR) [2,3]. Here the current density is large as a result of strong field gradients. The absence of flux freezing in the DR allows magnetic field annihilation and outflow perpendicular to the inflow. These regions are shaded in Fig. 1. Rapid, steady state reconnection maintains the height of the DR, $h \ll L$, where L is the length scale of the overall variation in the magnetic field.

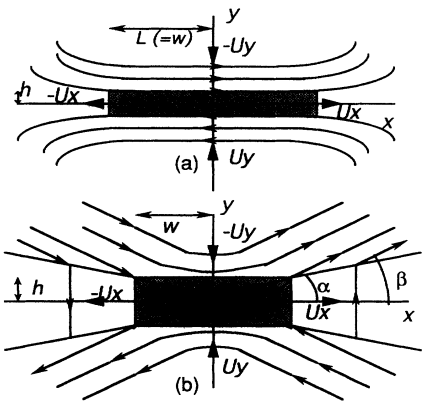

FIG. 1. (a) Relativistic Sweet-Parker reconnection. (b) Relativistic Petschek reconnection. Small arrows indicate field direction and large arrows indicate flow. The dissipation regions are shaded. For the Petschek model, the macroscopic field gradient length L is not shown because $L \gg w$.

The important difference between the Sweet-Parker [2] (SP) and the Petschek [3] (PK) models of Fig. 1 is that the length of the DR, w, satisfies $w \sim L$ for SP and $w \ll L$ for PK. In the PK outflow, the field reconnects, and its tension thrusts the plasma away from the x point along the x axis. Most of the energy conversion takes place across standing shocks which stem from each corner of the DR. The *length* of the DR is then determined by the distance from the origin for which the Alfvén velocity associated with the normal component of the proper frame magnetic field is large enough to balance the inflow velocity.

For nonrelativistic flows, PK provides a faster rate of reconnection for a given outflow velocity than SP. We will show that in the relativistic regime, this feature is maintained for outflows $< c$. For extremely relativistic outflows, however, both can provide rapid energy conversion because the Lorentz contraction of the outflow density allows more plasma to flow through a given cross section. When the magnitude of the inflow magnetic energy density is larger than the rest energy density, the kinetic energy of the ejected plasma will be relativistic.

In this paper we assume that the collisional term dominates synchrotron radiation losses in the Boltzmann equation and that the charge density, mean velocity, and mean momentum vanish in the same frame. We denote quantities measured in this "proper frame" by a superscript $*$. For PK we also assume that the outflow field is very small compared to the inflow field, and that the inflow four-velocity is much less than the outflow four-velocity. These are mutually consistent assumptions.

We employ Ohm's law, the magnetic induction equation, and the continuity equation to obtain the steady state SP inflow velocity as a function of resistivity and outflow velocity by enforcing $w^* = L$. To obtain the PK solution, we then allow $w^* \ll L$, and must also use energy-momentum conservation and the inflow field solution to find the w^* which maximizes the inflow rate. We

0031-9007/94/72(4)/494(4)$06.00

work in Gaussian units.

Blackman and Field [4] show that Ohm's law for a relativistic pair plasma under fairly general conditions has the MHD form

$$F^{\mu\nu}U_\nu=\eta j^\mu, \tag{1}$$

where j^μ is the current density, $F^{\mu\nu}$ is the electromagnetic tensor, η is the resistivity, and U^μ is a frame four-velocity. We shall assume that the inflow and outflow velocities are nearly constant and uniform so that the inflow and outflow regions each have unique proper frames and field gradients occur only in the DR. Using (1) and Maxwell's equations, the inflow magnetic induction equation is given by

$$-\partial^2\mathbf{B}/\partial t^2+c^2\nabla^2\mathbf{B} =(4\pi\gamma_y/\eta)\{\partial\mathbf{B}/\partial t-\nabla\times[(-V_y\hat{\mathbf{y}})\times\mathbf{B}]\}, \tag{2}$$

where V_y is the magnitude of the inflow velocity and γ_y is its associated Lorentz factor. Let us approximate the derivatives over small scales by the inverse of their size scales. Thus, Δt is the time scale for flux dissipation and $\Delta x=h$, the thickness of the DR. From (2) we obtain

$$U_y\sim\eta c/8\pi\gamma_y^2h=\eta_{\rm eff}c/8\pi h^*, \tag{3}$$

where $U_y\equiv\gamma_yV_y$, and $\eta_{\rm eff}\equiv\eta/\gamma_y$.

For a relativistic plasma satisfying (1), the particle number conservation equation for steady flow is given by [4]

$$\partial(\rho^*U_i)/\partial x_i=0, \tag{4}$$

where ρ is the mass density. Integrating this over the four-volume gives

$$\int\partial_\mu(\rho^*U^\mu)d^4x=\int\rho^*U^\mu dS_\mu=\text{const}. \tag{5}$$

For the very small DR, in the 2D steady state, this implies

$$U_y/U_x=\Delta y^*/\Delta x^*=h^*/w^*. \tag{6}$$

To obtain the SP inflow velocity, we set $w^*=L$ in (6) and combine with (3) to obtain

$$U_y/U_x=(\eta_{\rm eff}c/8\pi U_xL)^{1/2}. \tag{7}$$

Since the maximum outflow velocity is the Alfvén velocity ($\sim c$) we have

$$\gamma_y^{1/2}U_{y_{\max}}/U_{x_{\max}}\sim(\eta c/8\pi L)^{1/2}\equiv R_o^{-1/2}, \tag{8}$$

where R_o is the magnetic Reynolds number of the outflow. This is the relativistic analog of the nonrelativistic result [2]. Note that (8) differs from a simple replacement of the nonrelativistic three-velocities by the four-velocities because of the factor $\gamma_y^{1/2}$ on the left-hand side. This factor enters because the Reynolds number is defined in terms of η not $\eta_{\rm eff}$.

However, as $\eta_{\rm eff}$ decreases, the number density of the outflow increases in proportion to γ_y. As a result of particle number conservation, this increase in outflow density allows more particles to travel through a given outflow cross section, increasing the rate of reconnection for a given DR thickness. Equation (8) indicates that this effect dominates the decrease in $\eta_{\rm eff}$. As the outflow velocity approaches c, small velocity changes greatly enhance this effect, so that although the γ_y may be $\ll\gamma_x$, the V_y can approach V_x. The energy conversion rate is thus increased in the relativistic regime. The top curve in Fig. 2 shows this result for SP. There we have plotted $V_{y_{\max}}$ as a function of $V_{x_{\max}}$ for a constant factor of $R_o/\gamma_x\sim8\pi L/\eta c\sim10^4$ ($R_o\gg1$ for astrophysical plasmas).

Equation (8) suggests that a smaller DR length would increase the inflow rate. If we relax the constraint that $w^*=L$, and instead allow the PK condition $w^*\ll L$, then the inflow field is bent as in Fig. 1(b). We must then solve for the optimal w^* that maximizes the ratio of four-velocities, subject to the PK boundary conditions (to be described later). The PK solution requires optimizing the geometry so that the gain in outflow field tension more than compensates for the difficulty of plasma inflow opposite to the inflow tension. As in the nonrelativistic regime, we expect this to improve the SP result. To generalize PK we must consider not only particle number conservation as for SP but also energy-momentum balance, and the field solution in the inflow region.

Total energy-momentum conservation is expressed as

$$\partial_\mu K^{\mu\nu}=-\partial_\mu\Theta^{\mu\nu}, \tag{9}$$

where $K^{\mu\nu}$ is the bulk energy-momentum tensor, and $\Theta^{\mu\nu}$ is the electromagnetic stress tensor. Since we assume that the variation in the inflow and outflow wedges takes place along the y and x directions, respectively, we will change the partial derivatives to total derivatives in considering these regions separately. We assume that magnetic energy is converted either to bulk flow or scalar pressure. The y component of (9) for the inflow region is then given by

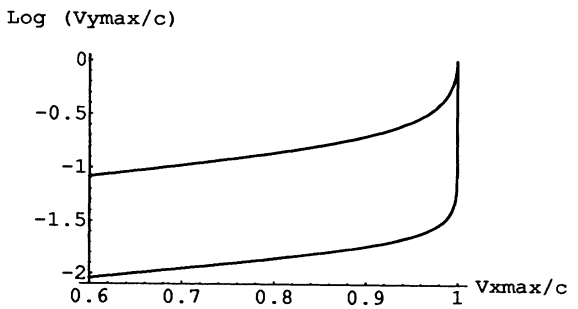

FIG. 2. $\ln V_{y_{\max}}$ plotted as a function of $V_{x_{\max}}$ in units of c, for $R_o/\gamma_x=10^4$. The top curve is the Petschek result [Eq. (29)], and the bottom curve is the Sweet-Parker result [Eq. (8)].

$$dP+U_y^2 d(\epsilon^*+P)+2U_y(\epsilon^*+P)dU_y=-(B_x/4\pi)dB_x\,, \tag{10}$$

where ϵ is the energy density, and P is the scalar pressure. dU_y cannot absorb the change in B_x since plasma flows in from both sides of the x axis. The change must be accounted for by an increase in fluid pressure. Then (10) becomes

$$dP+U_y^2 d(\epsilon^*+P)=-(B_x/4\pi)dB_x\,. \tag{11}$$

To proceed further we employ the ultrarelativistic approximation to the equation of state for low densities and high temperatures [5],

$$P=\epsilon^*/3\,. \tag{12}$$

Integrating (10) then gives

$$P_0=P_{\rm in}=B_L^2/8\pi(1+4U_y^2)\,, \tag{13}$$

where P_0 is the fluid pressure at the x point, and $P_{\rm in}$ is the fluid pressure in the inflow wedge far away from the DR, where $\mathbf{B}=B_L\hat{\mathbf{x}}$.

We assume that any change in magnetic field in the outflow wedge is small. The x component of (9) there is then

$$dP+U_x^2 d(\epsilon^*+P)+2U_x(\epsilon^*+P)dU_x=0\,. \tag{14}$$

Using (12) and integrating gives

$$\ln(P_0/P_{\rm ot})=\ln(1+4U_x^2)\,, \tag{15}$$

where $P_{\rm ot}$ is the pressure in the outflow wedge. Therefore

$$P_0/P_{\rm ot}=1+4U_x^2\,. \tag{16}$$

All of the magnetic energy is converted to plasma kinetic energy at the x point. The simplest case, and the one which maximizes the outflow velocity, is when all of the magnetic energy is converted into bulk kinetic energy. In this case, $P_{\rm ot}=P_{\rm in}$, and we can substitute (13) into (16) to obtain

$$U_{x_{\max}}^2=B_L^2/32\pi(1+4U_y^2)P_{\rm in}\,. \tag{17}$$

We assume that most of the change in $\mathbf{B}$ occurs within the DR so that outside, $\mathbf{B}=\nabla\psi$ and

$$\partial_i\partial^i\psi=0=\partial_\mu\partial^\mu\psi \tag{18}$$

in the steady state [6]. Define $r\equiv|\mathbf{r}|\equiv(x^2+y^2)$ and $\theta\equiv\tan^{-1}y/x$. Our PK boundary conditions are $\mathbf{B}=\nabla\psi=0$ at $r=0$, $\mathbf{B}=\nabla\psi=B_L\hat{\mathbf{x}}$ at $r=L$, and $B_\theta=0$ at $\theta=\beta$, where β is the angle between the x axis and the field in the inflow wedge shown in Fig. 1(b). The appropriate solution of Laplace's equation in polar coordinates [6] is

$$B_r=B_L(r/L)^{2\beta/(\pi-2\beta/\pi)}\cos(\theta-\beta)/(1-2\beta/\pi)\,, \tag{19}$$

$$B_\theta=B_L(r/L)^{2\beta/(\pi-2\beta/\pi)}\sin(\theta-\beta)/(1-2\beta/\pi)\,. \tag{20}$$

The presence of stationary shocks requires the relativistic Alfvén velocity associated with the proper frame field normal to the shock to balance the parallel component of the inflow velocity in the laboratory frame. For $h\ll w$, the angles are small, and this equality is given by

$$U_y^2=(\alpha-\beta)B_L^{*2}(w/L)^{2\beta/(\pi-2\beta)}/12\pi P_{\rm in}\,, \tag{21}$$

where α is the angle between the x axis and the shock shown in Fig. 1(b). Note that $B_L^{*2}=\gamma_y^2 B_L^2$, since $E_x=E_y=0$, and $V_y\perp B_L$. Then using (16), (17), and (21), we obtain in the small angle approximation

$$\gamma_y^{-1}g(U_y)=(8/3)^{1/2}U_{x_{\max}}(w^*/L)^{2\beta^*/(\pi-2\beta^*)}(\beta^*-\alpha^*)\,, \tag{22}$$

where $g(U_y)=U_y/(1+4U_y^2)^{1/2}$.

Equation (22) gives one equation relating U_y to $U_{x_{\max}}$. Let us obtain another from consideration of the field at the top center of the DR ($x=0, y=h, \theta=\pi/2$). From (17), (6), and (20) we have in the small angle approximation,

$$U_y/U_{x_{\max}}=\alpha^*(h^*/L)^{2\beta^*/(\pi-2\beta^*)}\,. \tag{23}$$

Equation (23) is the second equation for U_y as a function of $U_{x_{\max}}$. In the small angle limit, (22) and (23) give

$$\beta^*-\alpha^*=(3/8)^{1/2}\alpha^*/\gamma_y(1+4U_y^2)^{1/2}\,. \tag{24}$$

Plugging this into (22), we have

$$U_y=U_{x_{\max}}\alpha^*(w^*/L)^{2\beta^*/(\pi-2\beta^*)}\,. \tag{25}$$

Rearranging (24) we also have

$$0.77\le\alpha^*/\beta^*\le 1\,, \tag{26}$$

since $0\le V_y/c\le 1$. Thus α^* has a nearly constant relation to β^* over a full range of inflow velocities. We write

$$\alpha^*\sim k\beta^*\,, \tag{27}$$

where k is approximately constant. ($k=\frac{1}{2}$ in the nonrelativistic limit.) Using (3), (6), (25), and (27) we obtain

$$U_y/U_{x_{\max}}=R_o^{-2\beta^*/\pi}(k\beta^*)^{(1-4\beta^*/\pi)}\,. \tag{28}$$

Define $\bar{R}_o\equiv k^2 R_o$. Then maximizing the left-hand side as a function of β^* gives the PK result

$$U_{y_{\max}}/U_{x_{\max}}\sim\frac{k}{\ln\gamma_y+\ln[\bar{R}_o]}\,. \tag{29}$$

Figure 2 shows how (29) allows $V_{y_{\max}}$ to approach $V_{x_{\max}}$ for even smaller $V_{x_{\max}}$ than the SP result (8), since the constant factor of R_o/γ_x enters for PK only logarithmically. The combined rate enhancement effects of outflow tension and Lorentz contracted outflow density described earlier work together in the PK picture. Equations (29) and (8) indicate that steady state reconnection can maintain relativistic inflows for relativistic outflows, allowing a relativistic rate of magnetic energy conversion. We have not discussed the details of the DR which are more important to SP than PK, since the latter has a smaller frac-

tion of energy converted in the DR and depends only logarithmically on the resistivity.

We now discuss possible applications of these results to jets of active galaxies (AG). Part of the energy in jet lepton populations is likely produced by local acceleration processes in order to maintain a power law distribution over kiloparsec scales [7]. This *in situ* acceleration has been thought to be due to stochastic and diffusive shock acceleration [7]. However, relativistic perpendicular shock acceleration is only effective for e^+-proton-e^- plasmas when the proton to e^+ number ratio ≥ 0.1 [8]. Presently, it is difficult to argue that relativistic reconnection provides an alternative for pure pair plasmas since the spectrum of the reconnection outflow particles is not well constrained by the theory. We simply note that time scale for energy gain can be on the order of the synchrotron loss time.

With this in mind, we discuss an application which appeals to the formation of shocks from the reconnection outflow. Shock acceleration is a leading candidate to explain blazar jet knots [9] which are often observed at the jet edges and can appear to move superluminally. If the jet is composed of magnetically confined pair plasma, local instability (kinking, for example) induced reconnection could induce rapid outflow into the ambient medium, producing a shock. It is likely that the ambient medium contains ions as well as leptons [10] so that the outflow region would entrain ions. Acceleration by these shocks would be consistent with the work of Hoshino *et al.* [8].

Another possible role of relativistic reconnection is as an aid to the formation and radiative acceleration of pair plasma blobs. This could occur even in conjunction with magnetohydrodynamic models of AGN jets. Relativistic reconnection could allow for very swift production of these blobs if magnetic loops fly up and pinch off as the result of unstable loop configurations [11]. One radiative acceleration mechanism is the Compton rocket, based on Thomson scattering from an underlying source of photons [12]. This process is limited most strongly by a finite source size (due to radiation drag) and by cooling losses, which incur on the time scale of the bulk momentum gain, thus inhibiting acceleration. If the source of photons is strongly concentrated toward the nucleus of the AG, then relativistic reconnection in the blob can steadily maintain a *spatial* fraction of high energy electrons prolonging the effectiveness of bulk acceleration [12].

Finally, we make a general note that small scale reconnection near a large scale shock could provide the preacceleration required [7] for shock acceleration.

We would like to thank A. Loeb and R. Kulsrud for discussions.

[1] E. R. Priest, in *Basic Plasma Processes on the Sun*, edited by E. R. Priest and V. Krishan, IAU Symposium (Kluwer Academic, Norwell, MA, 1990).

[2] P. A. Sweet, Proc. IAU Symp. **6**, 123 (1958); E.N. Parker, J. Geophys. Res. **79**, 1558 (1957).

[3] H. E. Petschek, *AAS-NASA Symposium on Physics of Solar Flares* (NASA SP-50, 1964), p. 425.

[4] E. G. Blackman and G. B. Field, Phys. Rev. Lett. **71**, 3481 (1993).

[5] R. K. Pathria, *Statistical Mechanics* (Pergamon, New York, 1972).

[6] E. N. Parker, *Cosmical Magnetic Fields* (Oxford Univ. Press, New York, 1979).

[7] J. A. Eilek and P. A. Hughes, in *Beams and Jets in Astrophysics*, edited by P. A. Hughes (Cambridge Univ. Press, Cambridge, 1991).

[8] M. Hoshino *et al.*, Astrophys. J. **390**, 454 (1992).

[9] M. Lainela *et al.*, in *Variability of Blazars*, edited by E. Valtaoja and M. Valtonen (Cambridge Univ. Press, Cambridge, 1992).

[10] M. Begelman *et al.*, Rev. Mod. Phys. **56**, 255 (1985).

[11] B. C. Low, Annu. Rev. Astron. Astrophys. **28**, 491 (1990).

[12] S. L. O'Dell, Astrophys. J. **243**, L147 (1983); E. S. Phinney, Mon. Not. R. Astron. Soc. **198**, 1109 (1982).

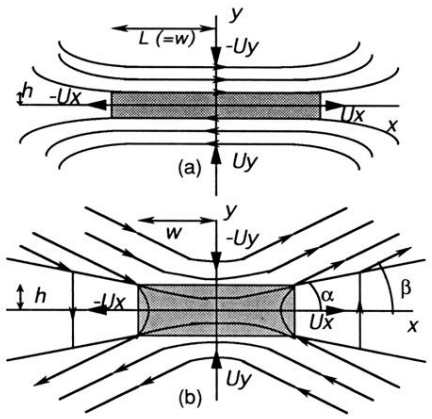

FIG. 1. (a) Relativistic Sweet-Parker reconnection. (b) Relativistic Petschek reconnection. Small arrows indicate field direction and large arrows indicate flow. The dissipation regions are shaded. For the Petschek model, the macroscopic field gradient length L is not shown because $L \gg w$.